SAMPEX: NASA's First Small Explorer Satellite

G. M. Mason[a], D. N. Baker[b], J. B. Blake[c], R. E. Boughner[d], L. B. Callis[d], A. C. Cummings[f], J. R. Cummings[f], M. E. Greenspan[a], D. C. Hamilton[a], D. Hovestadt[e], S. G. Kanekal[g], B. Klecker[e], R. L. Leske[f], X. Li[b], M. D. Looper[c], J. E. Mazur[c], R. A. Mewaldt[f], M. Oetliker[e], M. Scholer[e], R. S. Selesnick[c], E. C. Stone[f], T. T. von Rosenvinge[g], and D. L. Williams[f]

[a] University of Maryland, College Park, MD 20742
301-405-6203; mason@sampx3.umd.edu
[b] University of Colorado, Boulder, CO 80302
[c] Aerospace Corporation, Los Angeles, CA 90009
[d] NASA/Langley Research Center, Hampton, VA 23665
[e] Max-Planck-Institut, D-85748 Garching, Germany
[f] California Institute of Technology, Pasadena, CA 91125
[g] NASA/Goddard Space Flight Center, Greenbelt, MD 20771

Abstract — The SAMPEX satellite, an international collaboration with Germany, is the first in a series of small explorer missions that NASA began in 1989 to perform astrophysics and space physics investigations with small spacecraft launched on expendable launch vehicles. SAMPEX was launched from VAFB on a Scout rocket in July 1992, just 39 months after selection by NASA. Operating in an 82° inclination orbit with altitudes between 520 and 670 km, the 350 lb spacecraft has performed flawlessly since launch. The spacecraft bus was developed by the Small Explorer project at Goddard Space Flight Center. SAMPEX carries a payload of four scientific instruments that study particles originating at the sun, in the so-called anomalous cosmic rays, and in the magnetosphere. The SAMPEX instruments have sensitivities >100 times larger than previous low Earth orbit spacecraft, that have led to new discoveries such as a new radiation belt of interstellar material and rare hydrogen and helium isotopes trapped in the radiation belts. SAMPEX provides routine global maps of the magnetosphere, and has given new insights into the processes by which radiation levels through the entire magnetosphere can become greatly enhanced, leading to operating spacecraft anomalies. We give an overview of the SAMPEX scientific goals, instrumentation, and mission development approach.

TABLE OF CONTENTS

1. INTRODUCTION

Nearly five years after its launch into the current minimum of the solar cycle, the Solar, Anomalous, and Magnetospheric Explorer (SAMPEX) spacecraft has carried out a wide range of observations and discoveries concerning solar, heliospheric, and magnetospheric energetic particles seen from its unique vantage point in a nearly polar, low Earth orbit. Since almost all of the processes we are studying are driven or heavily influenced by the solar activity cycle, we have the opportunity to fully characterize the solar cycle dependence of a wide range of processes central to the goals of the NASA Office of Space Science's Sun-Earth Connections (SEC) theme. Over the next several years as the solar activity ramps up to its 11-year maximum, SAMPEX investigations will:

- survey the acceleration of relativistic electrons, measure their impact on the upper atmosphere, and determine their influence on atmospheric chemistry not only for solar minimum conditions but also for the much more complex solar active periods
- obtain samples of solar material from dozens of flares, compared with the handful observed during the declining phase of the solar cycle
- measure the anomalous component isotopic composition, trapping lifetime, and disappearance near solar maximum
- serve as a unique link in the chain of observatories put in place by NASA and its international partners to study space weather during the upcoming solar maximum.

Most of these investigations can only be carried out using SAMPEX's unique orbit and highly sensitive detectors, and cannot be accomplished with other operating or planned spacecraft.

SAMPEX investigations are addressing a very broad range of questions. We have carried out and reported to the scientific community major findings addressing the solar, anomalous, and magnetospheric particles for which the mission is named.

Since the Sun's activity cycle has profound influences on most NASA Sun-Earth Connection (SEC) questions, it is essential to carry out observations during both solar quiet and solar active periods if a scientific understanding of the processes is to be achieved.

0-7803-4311-5/98/$10.00

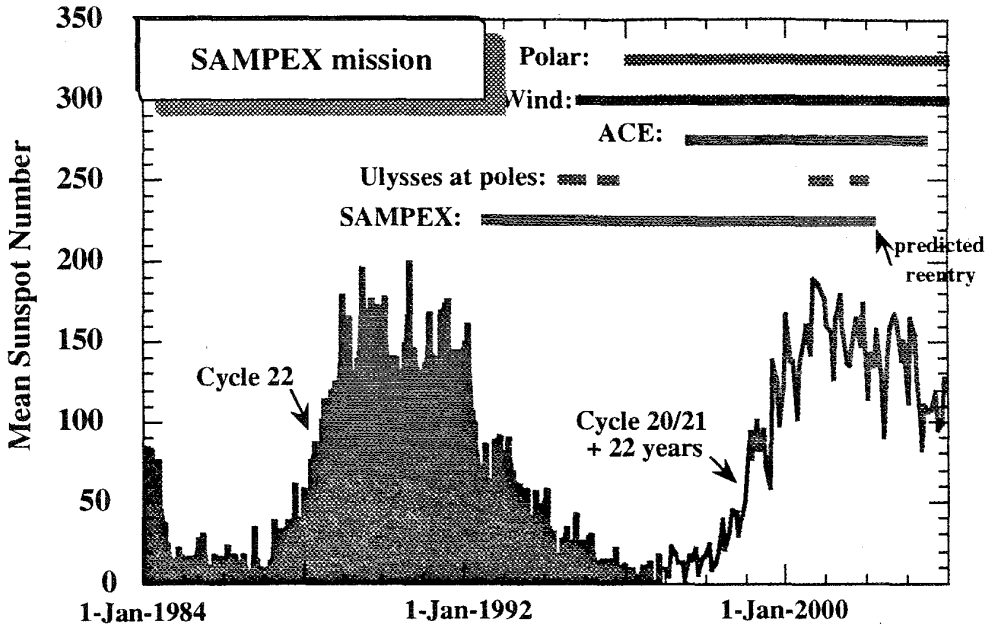

Figure 1 Solar sunspot numbers and spacecraft timelines through the next solar maximum.

Figure 1 puts the time-line of the SAMPEX mission in the context of the sunspot cycle. The figure also shows time-lines of some other SEC missions, showing that the scientific community has an opportunity to observe the upcoming solar maximum activity with a fleet of spacecraft with unprecedented capabilities. In the past year we have increased our emphasis on magnetospheric studies by greatly increasing the pitch angle coverage of SAMPEX. This was accomplished making use of the powerful on-board attitude control system to spin up the spacecraft to 1 RPM (vs 1 revolution for each 96 minute orbit previously).

The SAMPEX payload includes 4 scientific instruments, described in section 3:

Instrument	Primary Measurements:
HILT	anomalous cosmic ray charge state; electrons > 150 keV
LICA	low energy ions; kilovolt electrons
MAST	solar, galactic, and anomalous cosmic ray isotopes
PET	electrons > 400 keV; H, He isotopes

2. SCIENCE GOALS AND OBJECTIVES

Magnetospheric studies

Trapped Magnetospheric Electrons — long term observations The sources, redistribution processes, and loss mechanisms of radiation belt particles are primary issues in magnetospheric physics. High energy electrons hold special interest because of their ubiquity in the Earth's magnetosphere and their importance to other scientific and technological issues. These include dose and bulk charging effects in space vehicles in most Earth orbits, coupling to the Earth's middle atmosphere, and the understanding of acceleration processes in remote astrophysical objects. The SAMPEX instrumentation has given us new, unique insights into the behavior of energetic electrons in the Earth's radiation belts. The HILT, PET, and LICA sensors provide an unprecedented combination of sensitivity and time resolution. The SAMPEX nearly polar orbit and its short period provides many complete latitudinal and thus L value samplings per day.

A comprehensive view is provided in figure 2, which shows the PET >0.4 MeV counting rate, sorted according to L value versus time. The logarithm of the electron intensity level in each L bin has been color coded according to the reference bar at the right of the figure for all L values between 1.0 and 8.0. Numerous abrupt flux increases occurred in the outer zone (L > 2.5) throughout the multi-year period shown. Abrupt enhancements occur within a day, extend over a broad range in L and reach to high latitudes, often beyond L = 6 (geostationary orbit) [1] . The >1 MeV and the >3 MeV channels from HILT exhibit the same basic features. Even the slot region around L ~ 2.5, which separates the inner and outer zones, is often temporarily filled with electrons. Previous results [2] suggested that the slot region is normally filled only during major geomagnetic storms. The SAMPEX data show more frequent filling.

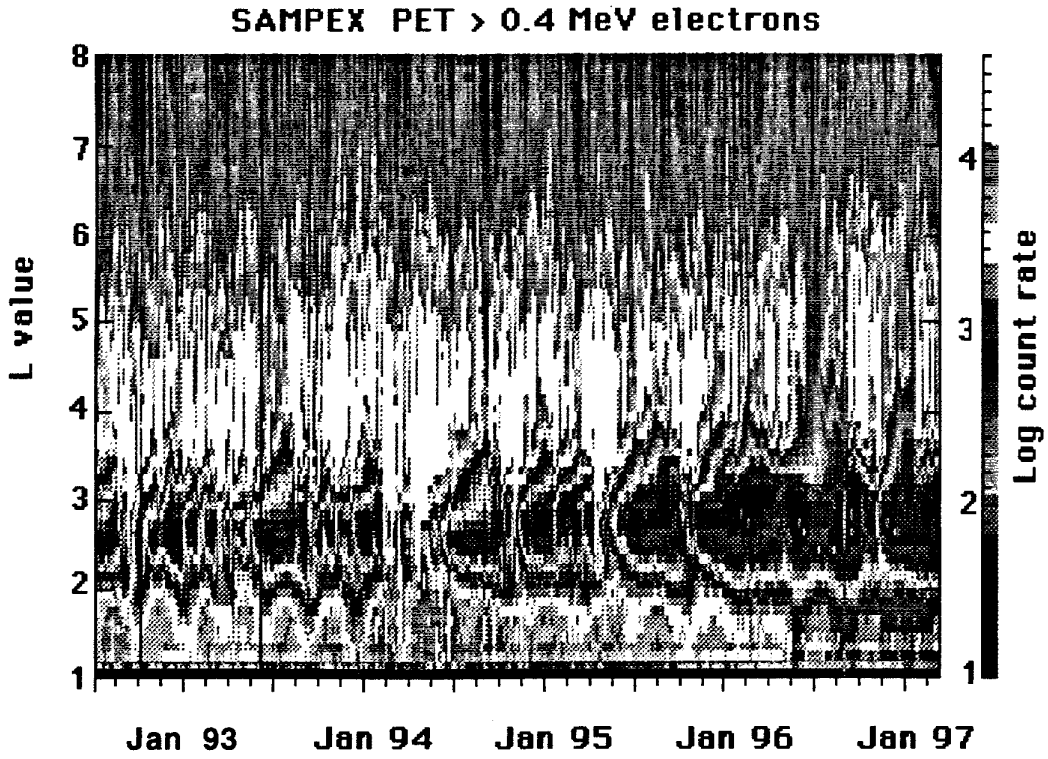

Figure 2 PET survey of >400 keV electrons arranged by L value vs time. Note the sharp flux increases that cover L values from ~3 to ~7.

SAMPEX data show the remarkable variation in electron properties as one goes to the heart of the outer radiation belt at L=4. These multi MeV electron fluxes vary by factors of 10-100 on time scales of a day. The fluxes correlate with high speed solar wind streams, peaking a day or two after the solar wind speed peaks upstream of the magnetosphere [3, 1, 4]. The maximum correlation between the high speed streams and radiation belt fluxes occurs with an increasing time delay for higher energies and lower L values [5]. Figure 3 shows HILT data from 15 May 1993 to 1 February 1994 (Days 500-763 of 1992). It is evident that the outer zone electrons exhibit very prominent flux peaks around Days 600, 680, and 750. These relativistic electron enhancements were associated with major spacecraft operational problems at geostationary orbit on January 20, 1994 including the loss of attitude control on Intelsat-K, and failure of the momentum wheel controls on the Anik E1 and E2 spacecraft [4] .

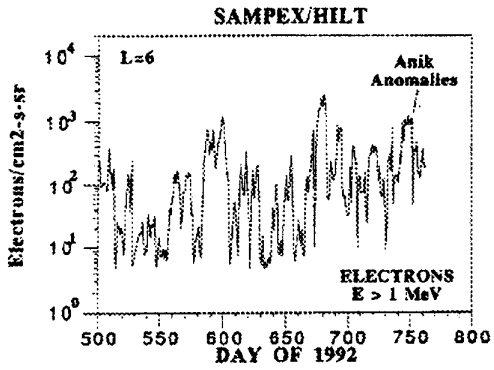

Figure 3 Outer zone electrons from HILT at L = 6 show large variations and correlation with spacecraft anomalies [4].

Coupling of magnetospheric precipitating electrons to the middle atmosphere — In the area of Earth sciences, there has been a long-term effort to understand the natural variation of the middle atmospheric chemical species important to the maintenance of global O_3. Among these species, the oxides of nitrogen (NO_y) are particularly important since they lead to the catalytic destruction of O_3. These natural variations must be understood in order to unambiguously assess the effect of man's activities on O_3. Such knowledge is critical since O_3 shields Earth from harmful UV radiation and is crucial in establishing the thermal structure of the stratosphere and, hence, its dynamic climatology.

Of particular interest is the effect of solar activity on this natural variability. It is well known [6] that variations in the Sun's UV flux modulate stratospheric O_3. It has been suggested [7, 8] that stratospheric O_3 may also be affected by the formation of mesospheric NO due to precipitating energetic electrons followed by advective transport of the NO into the stratosphere (during the late fall, winter, and spring) where it may enhance the catalytic destruction of O_3.

Several studies [9-12] have shown that relativistic electron precipitation events can, through energy deposition, provide the dominant ionizing process between 50 and 120 km. It is known that such ionizing processes can lead to the formation of oxides of nitrogen (NO_y) in the middle atmosphere. Figure 4 illustrates the daily NO_y formation derived from precipitating electron fluxes in the northern hemisphere for $L > 5$ shown as a function of altitude and time for 1994 [13]. It is shown as a percentage of the average of many NO profiles (between 45 and 65° latitude) observed by the UARS Halogen Occultation Experiment (HALOE) for $25 < Z < 130$ km. Figure 4 illustrates both the rapid and longer-term variations of the NO_y formation rate.

Crucial to a firm resolution of this issue are the synergistic observations of energetic electrons from low Earth orbit together with NO observations by HALOE through solar maximum. HALOE is planned to continue operating indefinitely. SAMPEX observations through solar maximum will allow a quantitative evaluation of this potentially important, highly interdisciplinary, and little recognized solar terrestrial coupling mechanism. Confirmation of this coupling would be seminal since it would open the door to many interesting interdisciplinary studies linking solar, space, and atmospheric physics.

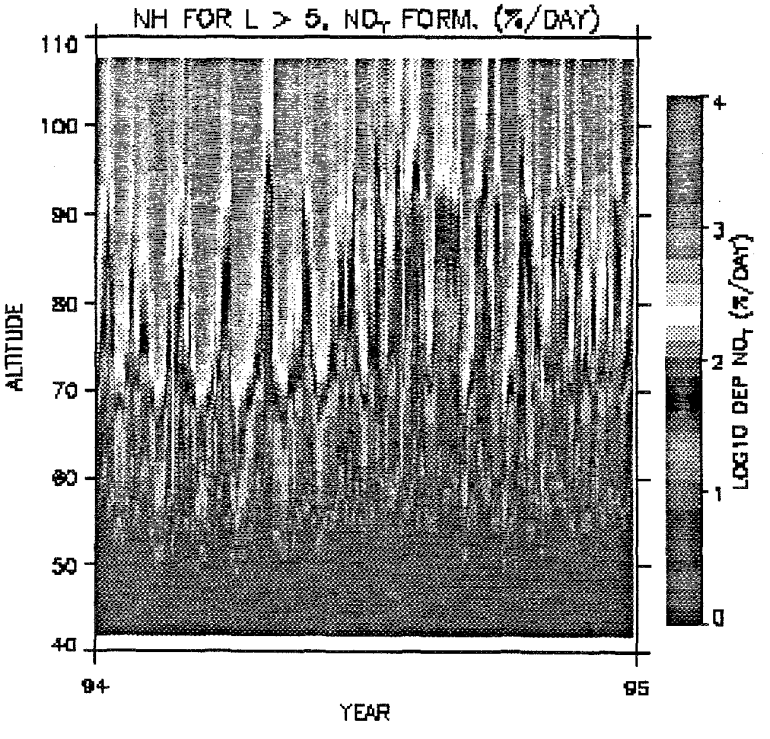

Figure 4 Altitude-time variation of daily NO_y formation expressed as a percentage of an average reference NO profile observed by HALOE.

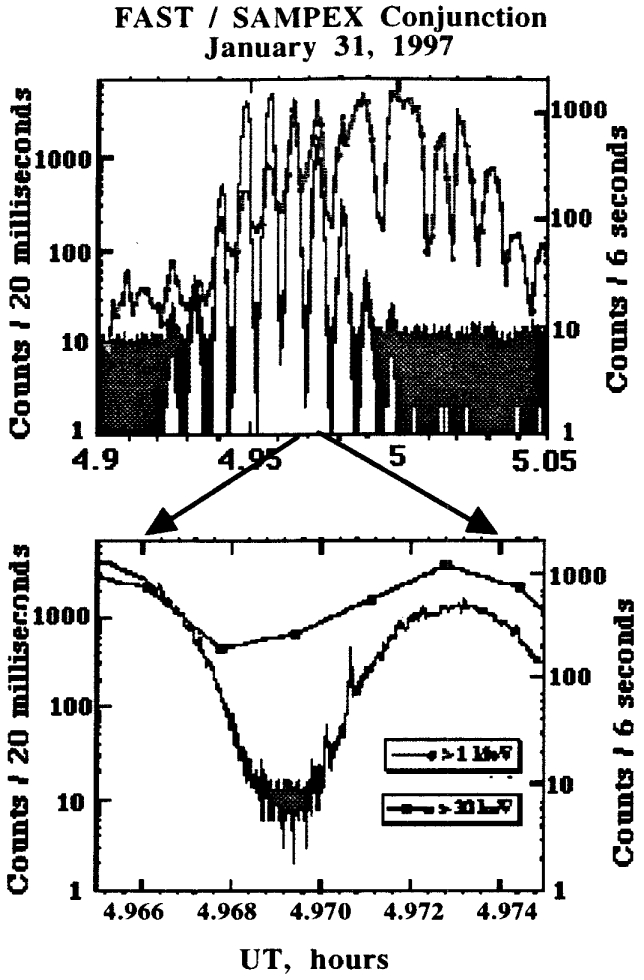

Figure 5 SAMPEX electron counting rates above 30 keV and 1 MeV near the time of a SAMPEX/ FAST conjunction. *Upper panel:* 6 minute interval; *Lower panel:* 36 sec. interval

In addition to providing support to UARS and POLAR investigations, SAMPEX also is making coordinated measurements with FAST (Fast Auroral SnapshoT Explorer). Besides the relativistic electron measurements mentioned above, the LICA instrument aboard SAMPEX also detects the integral electron flux above 30 keV. The geometric factor of this electron channel is several orders of magnitude larger than the usual auroral plasma analyzer. SAMPEX provides measurements outside of the energy and dynamic range of the FAST instrument complement. Figure 5 shows an example of LICA and HILT observations during a FAST-SAMPEX conjunction. The amplitude of the count rate modulation is a measure of the anisotropy of the electron pitch-angle distributions. It can be seen that just before 5 UT, the > 30 keV electrons became nearly isotropic over the upper hemisphere, indicating strong precipitation. The lower panel of figure 5 shows an expanded time scale. It can be seen that bursts of > 1 MeV electron precipitation are superimposed upon the mean electron intensities. Measurements of this kind are available only from SAMPEX; they are unique to date and most likely will remain so for the foreseeable future.

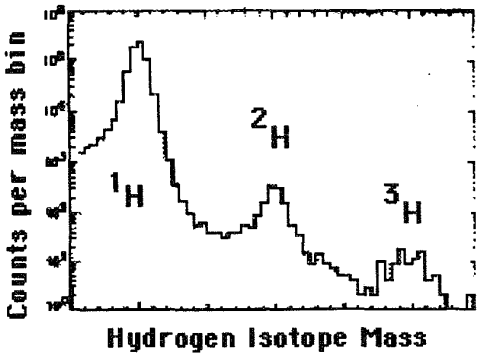

Figure 6 PET mass histograms of trapped H, ^{2}H, and ^{3}H.

Trapped H and He isotopes — SAMPEX is the first mission to explore the isotopic composition of the radiation belts and it has discovered that the rare isotopes ^{2}H, ^{3}H, and ^{3}He provide a tracer of the origin and evolution of trapped ions, just as they do in other energetic particle components such as Solar Energetic Particles (SEP) and Galactic Cosmic Rays (GCR). Using MAST, we have discovered [14] that about one-half of the 8 to 15 MeV/nuc He at L~1.2 is actually ^{3}He; this is surprising since ^{3}He/^{4}He ~0.0004 in the solar wind and ~0.00014 in the Earth's atmosphere. PET also observed both ^{2}H and ^{3}H at L=1.2 (see figure 6), with abundances of ^{2}H/^{1}H ~ 0.01 and ^{3}H/^{1}H ~ 0.001 [15].

Although there could be several possible origins of trapped ^{3}He, the presence of trapped ^{2}H and the radioactive isotope ^{3}H confirms these rare isotopes must originate in collisions of high energy protons in the inner Van Allen Belt with He and O atoms in the upper atmosphere. Our model of this process [14] takes account of the energy spectra of trapped protons, the composition of the upper atmosphere, and cross sections and kinematics for producing ^{2}H, ^{3}H, and ^{3}He from p+^{4}He and p+^{16}O reactions. The results are in reasonable agreement with the data.

Ring current neutral ions — Because it is beneath the Earth's radiation belts, the orbit of SAMPEX allows us to measure a trapped ion population whose origin is the high-altitude ring current. As the ring current decays after a geomagnetic storm, a large fraction of the particles become neutral. Some of these neutrals, no longer bound by the geomagnetic field, travel to the altitude of SAMPEX where they are ionized in the residual atmosphere and become trapped [16]. Figure 7 shows a global image of the counting rate of >770 keV protons measured with the LICA sensor for a 6-day period in April 1993. The ring current-associated particles mirror in a narrow band centered on the geomagnetic equator. Using the high sensitivity LICA measurements, we can follow their time evolution during geomagnetic storms. The SAMPEX 1-RPM spin mode initiated in 1996 combined with higher time sampling (1 sec) of the LICA count rates to be initiated in 1997, will enable us to answer more detailed questions about the origin and fate of this trapped particle population in the higher activity periods associated with the upcoming solar maximum.

Space Weather

Space weather involves the effects of solar and geomagnetic storms on technological systems both on spacecraft and on the ground. A particularly important problem is the degradation (and, sometimes, failure) of satellite subsystems that occur as spacecraft fly repeatedly through the Earth's radiation belts. It is crucial that satellite design engineers know accurately the fluxes, spectra, and time variabilities of trapped particle species so that components and subsystems can be designed to survive the radiation doses encountered. With its high sensitivity sensors and nearly polar low Earth orbit, SAMPEX is providing new insights into these issues.

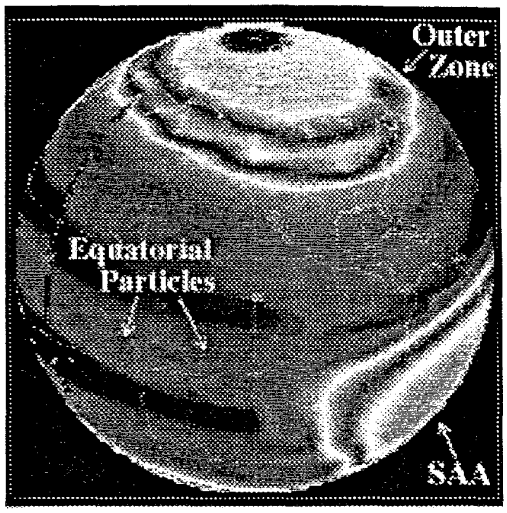

Figure 7 Average rate of >770 keV protons measured with LICA from 4/2/1993 to 4/7/1993. The faint band of particles near the geomagnetic equator originate as ring current neutral atoms.

As construction of the International Space Station (ISS) commences, space weather is more important than ever before.

Radiation belt model updates — PET observations have provided us with a long-term, intra-calibrated database of measurements of the protons of the inner radiation belt, from 19 to 500 MeV. This data set is well suited to constraining the low-altitude portion of new models of the inner-zone proton population, which are being developed to replace the old AP8 models. Such an updated model may include continuous solar-cycle phase dependence as opposed to the discrete, two-state AP8MIN/MAX model as well as details concerning the directional dependence of the flux.

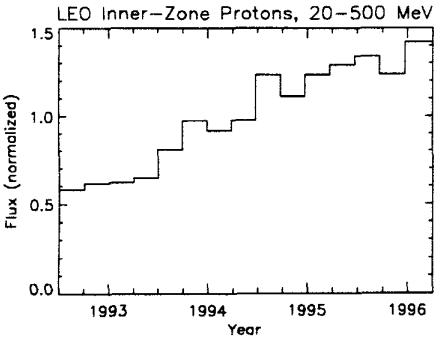

Figure 8 PET has observed a three-fold increase in inner-belt protons.

Figure 8 shows PET observations tracing a threefold increase in proton flux from start of mission through March 1996, and with an extended mission we could trace out the declining flux as increased solar activity heats and expands the upper atmosphere, thereby shortening particle lifetimes. We have shared the PET observations with colleagues at the Belgian Institute for Space Aeronomy (IASB/BIRA) for use in their efforts to construct a new model of the low-altitude inner zone, and we will continue working with them in this effort in an extended mission.

Space Station near-real time cutoffs — During large solar particle events, the fluxes over the poles may increase by many orders of magnitude. At lower latitudes, the Earth's magnetic field prevents low energy charged particles from getting through to low altitudes. The location of the transition, or cutoff, from the high radiation environment of the poles to the sheltered lower latitudes is easily detectable with SAMPEX during large particle events. Figure 9 shows the invariant latitude of the cutoff observed with SAMPEX proton and alpha particle rates for each orbit during the October/November 1992 SEP events. The geomagnetic activity index Dst is also shown for comparison. Note that the cutoff varies with time. Geomagnetic activity was not particularly severe during this event (Dst values can drop below -200 nT in major geomagnetic storms), yet the cutoff latitude changed by more than 5° in less than one day. Although the variation of the cutoff shows a good correlation with Dst, there are large differences during the passage of a shock (around day 307 in figure 9) when Dst actually lags the cutoff variations. Thus, even if Dst were instantly available or accurately predictable, it is no substitute for a direct measurement of the cutoff location during the most critical periods of rapid change.

Study of operational spacecraft anomalies — These anomalies can occur because of spacecraft charging as well as single event upsets (SEUs) and other such episodic phenomena. SAMPEX has already demonstrated its utility for understanding the occurrence of deep dielectric or "bulk" charging [4]. As very high energy electrons build up in the magnetosphere, spacecraft at many locations (especially in the outer magnetosphere) can suffer anomalies, or even failures, due to the electron environment. Figure 10 shows an example of this from the widely-reported January 1997 event associated with the loss of an AT&T communications satellite [18-20]. Also, as large solar energetic particle events become more frequent later in this solar cycle, we expect many more problems with energetic heavy ions causing SEUs on operational spacecraft. SAMPEX provides the ideal complement of sensors to monitor the electron and ion populations, and we offer the data and expertise of our team to help evaluate anomalies and failures. Thus, continuous data acquisition during this solar cycle can have important practical benefits.

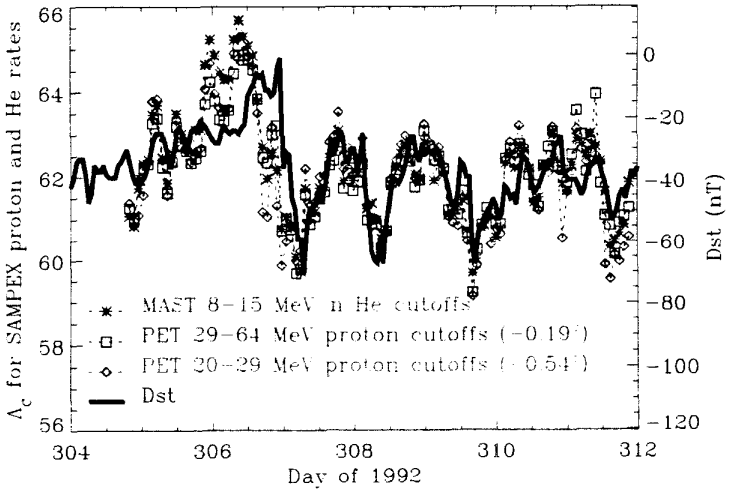

Figure 9 The location of the geomagnetic cutoff (in invariant latitude) vs time during the October/ November 1992 SEP events, measured on SAMPEX [17]. Arrow marks time of shock passage.

Solar Energetic Particles

Solar energetic particle ionization states — The ionization states of heavy ions measured in a number of large solar energetic particle (SEP) events [21, 22] have been found to be roughly consistent with equilibrium temperatures of a few $\times 10^6$ K, but with significant element to element differences. SEP charge states have provided some of the strongest evidence that in large ("gradual") flares the energetic particle seed population is the corona, rather than the much hotter ($>10^7$ K) site of the optical flare.

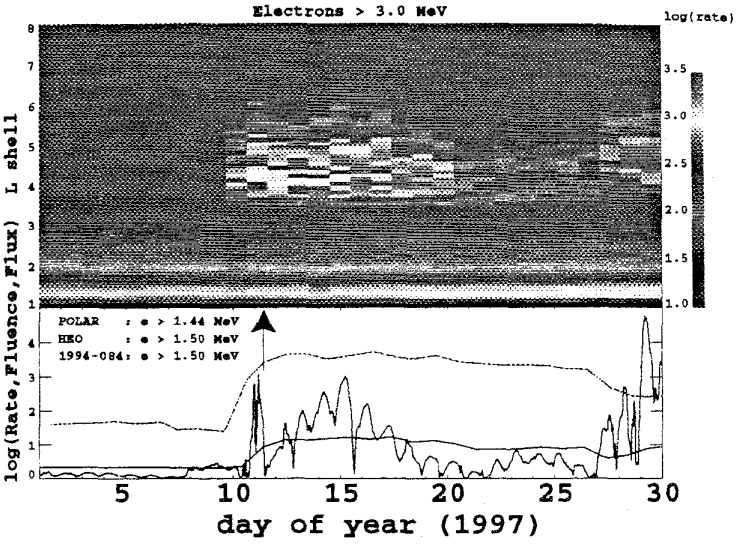

Figure 10 *Upper panel:* SAMPEX spectrogram of January 1997 period associated with the loss of the AT&T Telstar 401 satellite. *Lower panel:* POLAR and other spacecraft fluxes. *Arrow* marks time of Telstar 401 failure.

Instruments measuring solar particle charge states in interplanetary space using electrostatic deflection techniques (both prior to SAMPEX and on the upcoming ACE mission) are limited to the energy range near 1 MeV/nucleon. On SAMPEX, however, we have used the geomagnetic field to differentiate charge states, with a vastly enlarged energy range available for study. This makes it possible to extend charge state measurements to considerably higher energies, thereby probing important new aspects of the acceleration process and the nature of the acceleration regions [23].

Since the launch of SAMPEX in July 1992 through the present time (October 1997), only the solar particle events of Oct/Nov 1992 have been large enough to make good use of this approach. Selected measurements from LICA [24], HILT [25], and MAST [17] of the mean ionic charge states as a function of energy during these particle events are shown in Figure 11. For most of the observed elements, the mean charge states determined by SAMPEX are consistent at all energies with those measured directly in previous particle events around 1 MeV/nuc [26], with the largest exception being for iron. The LICA results, averaged over the energy range ~0.5-5 MeV/nuc, show a mean charge state of 11.04 ± 0.22 for Fe [24], while the average from Luhn [26] is 14.09 ± 0.09. The mean value rises to 15.18 ± 0.73 over the ~28-65 MeV/nuc energy interval of MAST, with some indication of an increase even across this interval. Although the cause of this energy dependence is not fully understood, the effect may be used to place limits on the particles' residence time in coronal loops [27].

Anomalous Cosmic Rays

A fundamental prediction of the interstellar neutral theory for the origin of ACRs [28] is that ACRs should be singly-charged, and there is now abundant evidence that the bulk of ACRs with ~10 MeV/nuc have an ionic charge-state of Q=1. Adams et al. [29], found Q = 0.9 (+0.3, -0.2) for 5 to 11 MeV/nuc ACR oxygen by comparing orbit-averaged fluxes inside the magnetosphere with interplanetary fluxes. HILT/SAMPEX measurements showed that >90% of 8 to 16 MeV/nuc ACR oxygen are singly-charged by measuring the latitude distribution of ACRs [30].

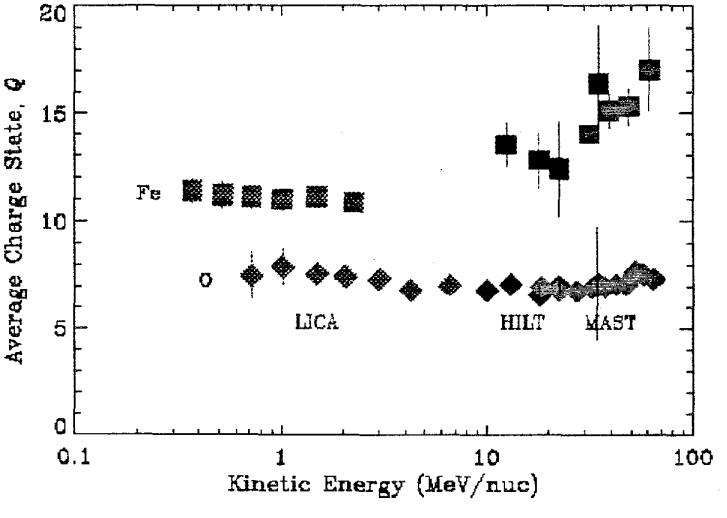

Figure 11 Deduced charge states as a function of energy for O and Fe measured by LICA [24], HILT [25], and MAST [17] during the Oct/Nov 1992 SEP event. Note the energy dependence in the mean iron charge state.

Recent measurements by both MAST and HILT have now extended these measurements to higher energy, again using the Earth's field as a magnetic spectrometer, and found a very surprising result: at energies >20 MeV/nuc the ACR oxygen charge state changes from singly ionized to charge states of Q=2, 3, and higher. We have shown that the fraction of multiply-charged ACRs serves as a clock for the acceleration process [31]. Assuming that the acceleration time scales with particle rigidity, and assuming a neutral hydrogen density of ~0.1 cm^{-3} at the termination shock, the observed fraction of multiply-charged ACRs implies that the acceleration process takes ~1 year to reach ~10 MeV/nuc. This time is consistent with theoretical limits published earlier [32, 33].

Recent results from both HILT and MAST show that ACR N and Ne are also multiply-charged at high energies, as illustrated by the Ne data in Figure 12. It is clear that the charge-state composition of ACRs is much more complex than previously assumed. Data such as these provide a unique opportunity to study an example of a shock acceleration process that occurs very close by on an astrophysical scale, but that most likely also occurs elsewhere in the Galaxy on larger scales. Extension of SAMPEX studies through the remaining solar minimum period will improve the statistical accuracy of these studies, particularly for the rarer species, and it will allow us to use the geomagnetic filter to trace the ACR flux at 1 AU through solar maximum for the first time.

Trapped Anomalous Cosmic Rays (ACR) — SAMPEX provides the only continuous measurements of the ACR belt, which we located [34] shortly after launch (see figure 13). However, the low data rates require long data collection periods for statistically significant results. Extending these beyond the years that were available for initial studies will provide significant improvement in our knowledge of this particle population, particularly for the rare elements and isotopes. The correlation of interplanetary and trapped fluxes during the declining phase will help estimate the trapping lifetime. It will be interesting to see if the belt disappears below the level of detectability.

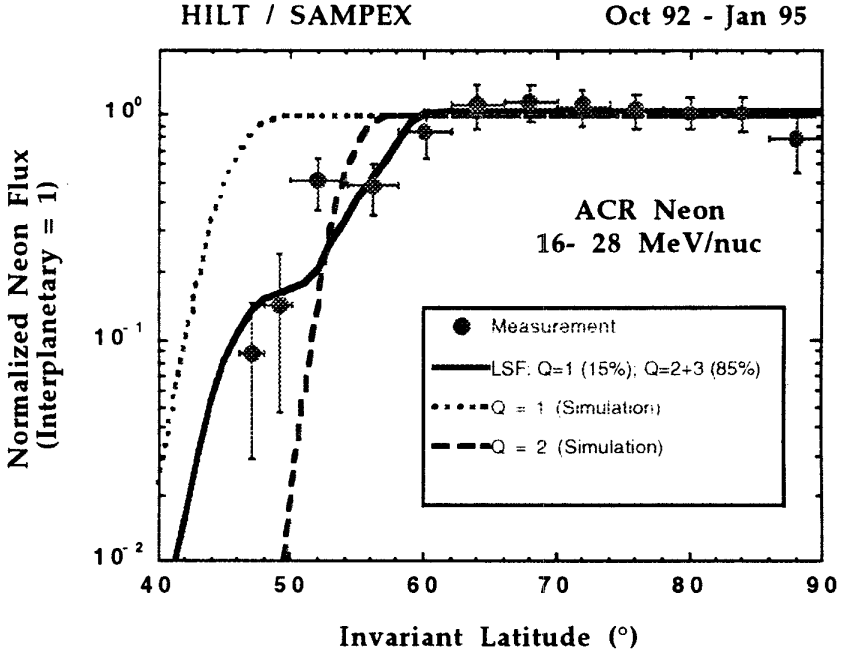

Figure 12 Latitude distribution of ACR neon (16-28 MeV/nuc) measured by HILT, along with a fit to the distribution including charge states 1, 2, and 3. The measured distribution at low energies (9 -16 MeV/nuc, not shown) is consistent with > 85% of Ne being singly ionized.

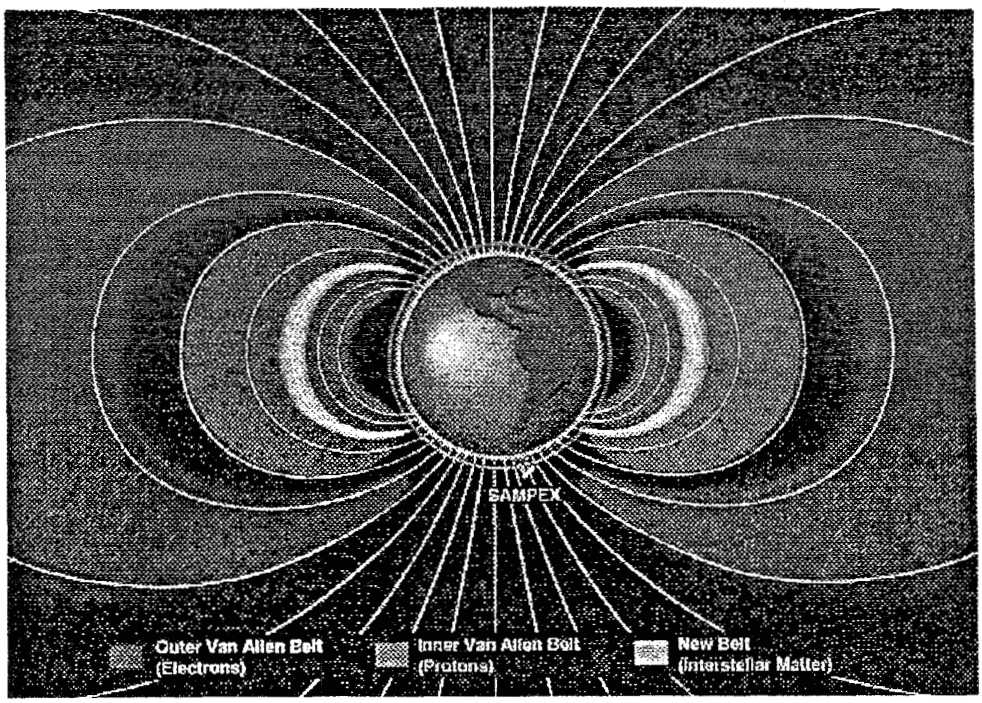

Figure 13 SAMPEX discovered the location of the ACR radiation belt.

3. INSTRUMENT DESCRIPTIONS

The SAMPEX instrument complement consists of four sensors:

- HILT — the Heavy Ion Large Telescope
- LICA — the Low Energy Ion Composition Analyzer
- MAST — the Mass Spectrometer Telescope
- PET — the Proton/Electron Telescope

The instruments use a combination of techniques to identify ions and electrons. MAST, PET, and HILT all rely principally on *dE/dx vs E* measurements carried out in solid state detectors and (in the case of HILT) flow-through proportional counters and drift chambers. LICA is a time-of-flight mass spectrometer. The overall range of particle response is summarized in the table below. Detailed instrument descriptions are given in separate subsections which follow (see also [35-40]).

Combined overall instrument parameters and energy ranges are in Table 1. The average science data rate is currently 30 Mb/day; peak: 50 Mb/day.

Table 1 Combined instrument responses

typical species	energy range	geometry factors (different instr.)
electrons	>25 keV	50 cm^2 sr.
relativistic electrons	0.4 - 30 MeV	0.3-100 cm^2 sr.
protons	0.76-250	0.3 - 14 cm^2 sr.
He	0.45 - 350	0.3 - 60 cm^2 sr.
C	0.44 - 210	0.6 - 60 cm^2 sr.
Fe	0.21 - 450	0.6 - 60 cm^2 sr.
Isotope range	Z = 2 - 28	0.6 - 14 cm^2 sr.
Element range	Z = 1- 28	0.6 - 60 cm^2 sr.
count rate resolution	electrons, protons	10 ms minimum
	other species	**6 s (typical)**

The Heavy Ion Large Telescope — HILT

The HILT sensor is designed to measure heavy ion elemental abundances, energy spectra, and direction of incidence in the mass range from helium to iron and in the energy range 4 to 250 MeV/nuc. With its large geometric factor of 60 cm^2 sr. the sensor is optimized to provide compositional and spectral measurements for low intensity cosmic rays, i.e. for small solar energetic particle events and for the anomalous component of cosmic rays.

The schematic diagram of HILT in Figure 14 shows the main sensor components: a three element ion drift chamber with thin aluminum entrance window (40 μm), followed by an array of 16 solid state detectors (SSD) and 16 CsI scintillation counters which are embedded in a plate of PERSPEX material and viewed by 4 light sensitive silicon diodes. The entrance foil serves as part of the gas enclosure and, in combination with two additional aluminum foils (2 x 20μm), as a shield against micrometeoroid impacts. The three elements of the ion drift chamber are the front proportional counter (PCF), the ionization chamber (IC) and the rear proportional counter (PCR). Typical energy ranges and geometrical factors are listed in Table 2.

The element or mass analysis is based on the combination of a multi dE/dx measurement in the position sensitive proportional counter and ionization chamber system with the measurement of residual energy in the SSD detector array and the CsI crystal unit. The direction of incidence is derived from position measurements with PCF and PCR, from the drift time of electrons (PCF), and from information on the SSD detector triggered. With the measurement of particle energy, mass, and direction, in combination with the spacecraft position and attitude in the low altitude polar orbit, it is possible to infer the ionic charge of the ions from the local cutoff of the Earth's magnetic field.

In addition to heavy ion measurements, HILT also provides measurements of electrons with energies > 15 keV and > 1 MeV with some directional information from the four rows of solid state detectors, and very high sensitivity (≈ 100 cm^2 sr. at 1 MeV) and time resolution (≈10 ms).

The gas supply of the drift chamber - proportional counter

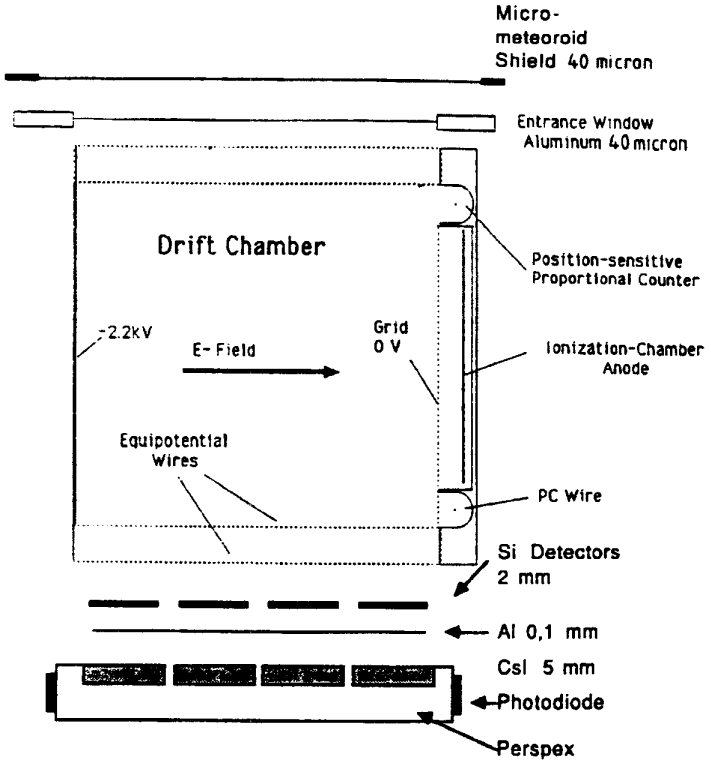

Figure 14 Schematic cross section of HILT sensor.

system limited the full operation of the sensor to about 1000 days. The last data taken with the proportional counter was in November 1995. Then, after letting the chamber outgas for a sufficiently long period, HILT was switched to its

Table 2 — HILT energy ranges for selected species

Element	Energy Range (MeV or MeV/nuc) Normal Mode (isobutane on)	Energy Range (MeV or MeV/nuc) High Energy Mode (isobutane off)	Geometry factor (cm^2sr)
electrons	>0.15	—	10
electrons	> 1.0	> 1.0	100
^{4}He	4.3 - 38	20 - 40	60
^{16}O	8.2 - 200	42 - 200	60

"High Energy" mode of operation in March 1996. In this mode the coincidence logic of the sensor is changed by command, recovering the > 1 MeV electron rates and high energy ions (see Table 2).

The Low Energy Ion Composition Analyzer — LICA

The Low Energy Ion Composition Analyzer (LICA) measures ion fluxes over the charge range from He through Ni from about 0.35 to ~10 MeV/nuc. A schematic cross section of the LICA telescope is shown in Figure 15. The instrument is a time-of-flight mass spectrometer that identifies incident ion mass m and energy by simultaneously measuring the time-of-flight t and residual kinetic energy E of particles that enter the telescope and stop in one of the array of four Si solid state detectors in the telescope. The time-of-flight is determined by START and STOP pulses from chevron microchannel plate (MCP) assemblies that detect secondary electrons that are emitted from the entrance foil and the front surface of the solid state detector, respectively, when the ion passes through them. These secondary electrons are accelerated to ~1 kV and deflected onto the MCPs by electrostatic mirrors. The design of the secondary electron optics yields isochronous flight paths for all secondary electrons emitted normally from the foils or detector surface. The measured energy $E = 1/2mv^2$, and the velocity $v = L/t$ (where L is the path length in the telescope) are combined to yield the mass of the ion $m = 2E(t/L)^2$, and the energy per nucleon E/M inside the telescope. The ion incident energy is obtained after correcting for the energy loss in the entrance foils. Energy ranges for major elements, and triggering efficiencies near 1 MeV/nuc are listed in Table 3. The instrument geometry factor for ion events is 0.58 cm^2 sr.

HILT Status — operating in high energy mode since March 4, 1996. Primary science data in high energy mode is electrons > 150 keV.

Because of the high event rates observed by LICA in large flares, it is not possible to transmit all particle information within available telemetry allocations. Two types of information are therefore returned: first, detailed pulse-height-analysis (PHA) data at a rate of up to 10 events/sec, and second, fast discriminator counting rates which allow normalization of the fluxes. On-board event gate logic examines all ions triggering the system, and in the case of PHA data makes a priority selection to prevent H or He nuclei from dominating the telemetry in active periods. High mass resolution analysis is done on the ground using the ion trajectory information telemetered with the PHA data. Mass histograms are formed for selected energy ranges, with the relative abundance of each species determined from the population at the appropriate mass bin in the histogram. Since LICA has multi-parameter analysis, it is possible to identify and correct for residual background in the instrument, an essential feature for identifying a broad range of ions with widely differing abundances.

LICA status — LICA is in excellent operating condition; start MCP gain degradation due to radiation belt passages is corrected by routine bias adjustments every 40 days.

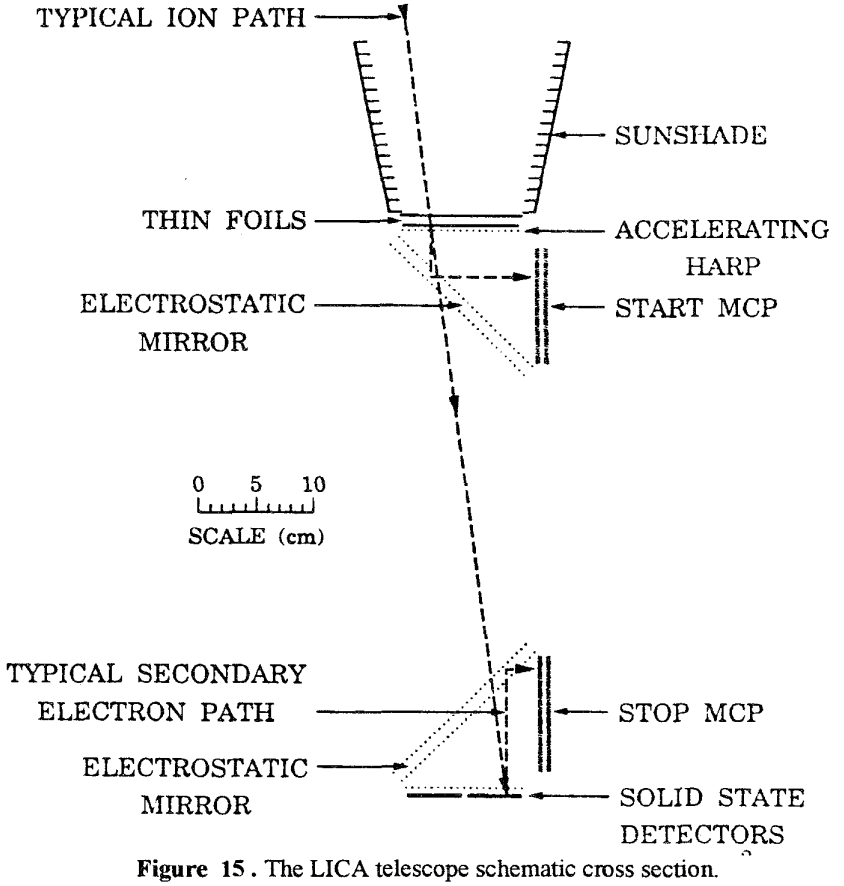

Figure 15. The LICA telescope schematic cross section.

Table 3 — LICA energy ranges for selected species		
Species	Energy Range (MeV/nuc)	Triggering Efficiency (%)*
^{1}H	0.76 - 6.05	~1
^{4}He	0.50 - 6.57	6
^{12}C	0.49 - 10.7	64
^{16}O	0.48 - 8.25	67
^{20}Ne	0.46 - 6.79	71
^{28}Si	0.39 - 5.05	78
^{56}Fe	0.21 - 2.87	79

*Near 1 MeV/nuc

The Mass Spectrometer Telescope — MAST

MAST is designed to provide high resolution measurements of the elemental and isotopic composition of energetic nuclei from He to Ni (Z = 2 to 28) over the energy range from ~10 to several hundred MeV/nuc. Over the geomagnetic poles MAST has been measuring the composition of both GCR and ACR nuclei during solar quiet times, and the isotopic composition of solar energetic particles during large solar events. Within the magnetosphere MAST has been measuring the spatial and pitch angle distributions, and the composition and energy spectra of trapped ACR nuclei, and it has discovered that in the inner radiation belt at L=1.2 the usually rare isotope ^{3}He actually exceeds ^{4}He in abundance. Studies with MAST have also used the Earth's magnetic field to measure the ionic charge state composition of solar energetic particles to energies >50 MeV/nuc, and to extend the energy spectrum of ACR nuclei to ~100 MeV/nuc.

The MAST telescope (see Figure 16) is composed of an array of silicon solid state detectors of graduated thicknesses, including four position sensitive detectors (PSDs) that measure the trajectories of incident nuclei in addition to their energy loss. The upper section of the telescope is composed of six surface-barrier devices labeled M1 through D2. The lower section has eight lithium-drifted (LiD) silicon wafers combined electronically into five detectors (labeled D3 to D7). Each of the LiDs has an annular guard region (G) that permits discrimination against events that exit or enter through the side of the detector stack. The central regions of all detectors except D7 are pulse-height-analyzed. Resolution of isotopes in MAST is accomplished by the standard *dE/dx vs.* residual energy technique, using anywhere from 4 to 10 individual measurements of energy loss for stopping nuclei. The telescope geometry factor is energy

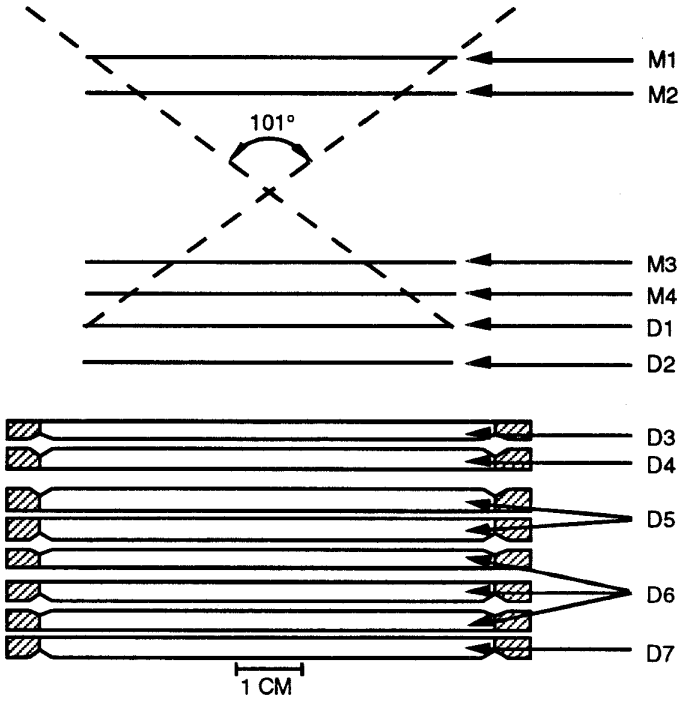

Figure 16 Cross section of the MAST telescope.

dependent, with a typical value of 10.6 cm^2 sr. near the middle of the detector stack.

The Proton / Electron Telescope — PET

The Proton Electron Telescope is providing measurements of energetic electrons and light nuclei from a variety of sources. PET is an all solid-state system that measures the intensity variations and energy spectra of electrons from ~0.4 to ~30 MeV and H and He nuclei from ~19 to ~300 MeV/nuc. Isotope resolution of H and He extends from ~19 to ~64 MeV/nuc.

As SAMPEX scans all local times and geomagnetic cutoffs over the course of its orbit, PET electron measurements have been used to track the response of outer zone electrons to high speed solar wind streams, to characterize the rich time structure of precipitating relativistic electron events; and to study the decay of the relativistic electron belt created during the intense geomagnetic storms of March, 1991. PET electron studies are also being used to examine whether the production rate of odd nitrogen and hydrogen molecules in the middle atmosphere by precipitating electrons is sufficient to affect O_3 depletion. In addition, PET measurements of energetic nuclei have been used to measure the abundance of deuterium in the inner radiation belt, to provide new maps of inner belt protons, and to support studies of the charge states of solar energetic particles. This rich variety of applications of PET data complements studies of composition and time variations of energetic heavy (Z>2) nuclei on SAMPEX by LICA, HILT, and MAST.

The PET telescope, shown in Figure 17, consists of a stack of 12 Li-drifted silicon detectors (combined electronically as P1 to P8), with combined thicknesses ranging from 2 to 15 mm. The telescope was originally designed to measure H, He and electrons in interplanetary space on the US spacecraft for the ISPM mission (now Ulysses). It is therefore not optimized for the magnetospheric studies of either electrons or nuclei, and considerable effort has therefore been invested to understand the instrument's operation in the harsh environment of the radiation belts.

The electron response of PET was calibrated prior to launch with a variety of beams from 0.3 to 27 MeV at the EG&G Santa Barbara linear electron accelerator. These calibration data have since been supplemented by Monte Carlo simulations of the instrument response (e.g., Looper et al. 1994). These calibrations have been used to develop several independent approaches to deriving electron spectra from PET.

Instrument Status — failure (July 1992) of ADC for highest energy electrons reduced upper energy range by ~25%.

MAST Status — some detector noise reduces livetime; continues to have excellent mass resolution.

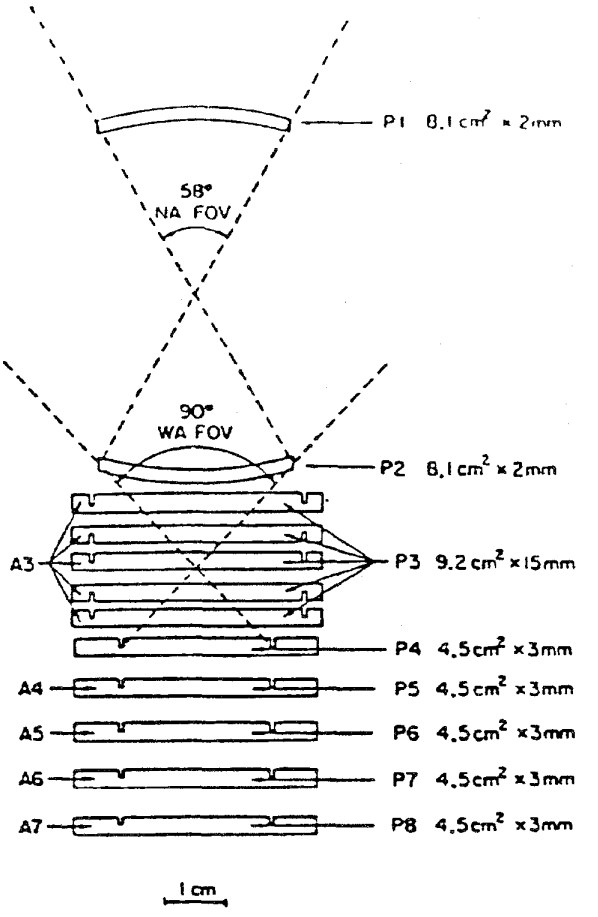

Figure 17 Cross section of the PET telescope.

Data Processing Unit (DPU)

The SAMPEX instruments connect to a single Data Processing Unit (DPU) which was built as part of the instrument [36]. The DPU collects all the instrument data, assembles it into data packets, and sends to the spacecraft data system for storage and later playback to the Wallops Island station. The DPU design is highly flexible, making it possible to adjust and optimize data collection and telemetry allocations in support of science investigations. Examples of changes already made during the course of the mission include:

- allocation of HILT high resolution rates to the SSD count rates
- allocation of HILT high resolution rates to SSD and front proportional counter
- modifying LICA, MAST, and PET maximum asynchronous pulse-height-readout rates to optimize data collection in solar particle events

- re-allocation of pulse-height-telemetry quotas between LICA, PET, and MAST to optimize telemetry use.
- modification of LICA rate collection to report 1-sec intervals (vs. 6 sec initially)

4. SPACECRAFT DESCRIPTION

The description below is extracted from Baker et. al. (*IEEE Trans. Geosci. Electr. and Remote Sensing*, SAMPEX special issue, vol. 31, May 1993). The status report was compiled from an analysis by the SAMPEX Flight Operations Team at Goddard Space Flight Center.

Spacecraft Configuration

The SAMPEX mission uses a spacecraft developed by the SMEX Project at the Goddard Space Flight Center. The spacecraft is required to provide the total support (power, data, thermal, structural, etc.) to four separate scientific instruments and their associated data processing unit. The spacecraft has been designed as a single string system. A system design was selected that uses proven design concepts and flight qualified or readily available hardware wherever possible. A Performance Assurance program with minimum paperwork, best experimenter judgment, and extensive bench testing has been implemented for the SAMPEX instrument payload. Within this resource-constrained package, there are many innovations including powerful onboard processors, optical fiber busses, solid state memory units, and a highly integrated mechanical design.

The SAMPEX spacecraft was designed to support a minimum mission duration of 1 year, with a mission goal of 3 or more years. Because the four-stage Scout launch vehicle could loft a very limited weight for this mission (< 372 pounds), the spacecraft systems were primarily designed in a single-string architecture. The SAMPEX mechanical system basically consists of a primary structure, a deployable solar array system, and a yo-yo despin system. SAMPEX is built up of machined aluminum plates which form a box-like structure that houses all of the spacecraft components (see Figure 18). An adapter ring on the bottom provides the interface to the Scout 200 E adapter on the fourth stage of the Scout launch vehicle. SAMPEX was designed to fit within the Scout 34-inch diameter heat shield.

The deployable solar arrays are configured in two symmetric wings. The arrays are deployed by a damped spring system which prevented the motion from imparting any severe loads on the structure. The arrays consist of four panels, associated deployment mechanisms, position monitors, cabling, gallium arsenide solar cells and cover glass. The solar array panels are fabricated from aluminum honeycomb and have solar cells bonded to them. Each array has two coarse sun sensors mounted on the upper and lower extreme corners.

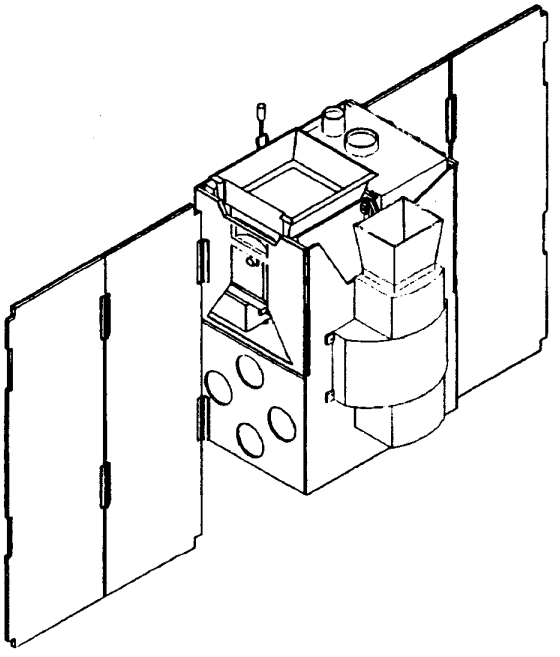

Figure 18*a* Mechanical design of the SAMPEX spacecraft and physical layout of scientific instruments

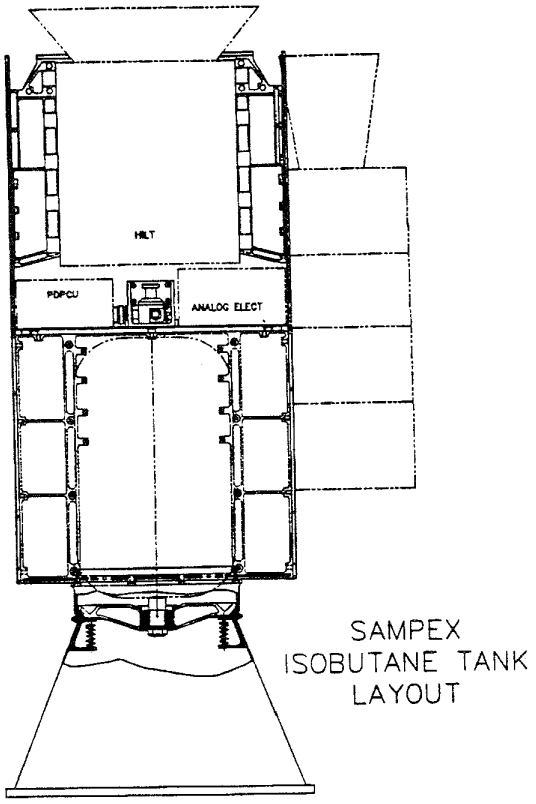

Figure 18*b* — side view of subsystems

Power subsystem

The power subsystem is a Direct Energy Transfer system providing an unregulated +28 volt direct current bus. Power is generated during the sunlight periods from the solar array paddles and stored in a nickel cadmium battery. Power is drawn solely from the batteries during eclipse periods. A shunt regulator is provided to dissipate excess array power.

The power subsystem supplies power to the spacecraft via three busses: the essential bus, the non-essential bus, and the pyrotechnic bus. The essential bus provides continuous power to spacecraft functions including the data system, the telemetry transponder, the heaters, the attitude control system, and the power distribution electronics. The non-essential bus provides power to the spacecraft instruments. The

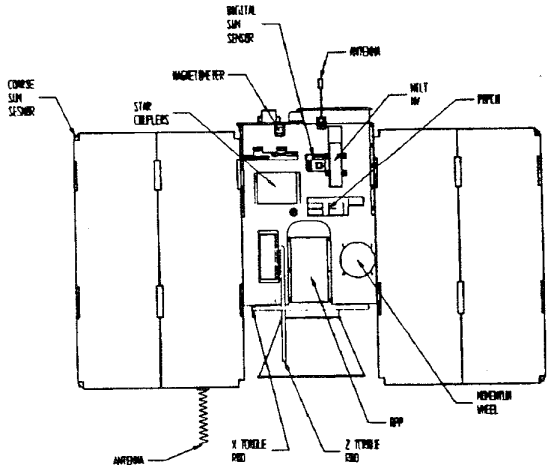

Figure 18*c* back view of subsystem layout

pyrotechnic bus provides unprotected battery power to fire the pyrotechnic devices. All three busses are routed to the power distribution unit for switching and fusing (where appropriate). The power subsystem includes an isolation relay to disconnect the non- essential bus in the event that the spacecraft is drawing excessive current, the battery is in undervoltage, or when the spacecraft goes into safehold. With the exception of the shunt drivers, all power subsystem electronics are designed in a single string, non-redundant configuration. The Power Distribution/Pyro Control Unit (PD/PCU) provides primary power distribution and fusing to other spacecraft subsystems, and control and power to the spacecraft's separation and deployment pyrotechnic devices.

The on-orbit average output power of the system is 102 watts with no solar array shadowing and minimum solar intensity at end-of-mission life. During the launch phase, with the spacecraft launched into a full sun orbit, the power system was capable of supplying 200 Watt-hours of energy. This is based on a 9 Amp-hour battery and an 80 percent battery depth of discharge.

Attitude Control System

The Attitude Control Subsystem (ACS) is designed as a solar-pointed/momentum-bias system. The SAMPEX spacecraft points at the sun while it rotates about the sunline once per orbit in order to position the instrument lines-of-sight in the zenith direction when overflying the poles. Pointing requirements for the selected experiments are met by choosing sensor, torquers, and system configurations from a standard set of electronics, sensors, and actuators. The ACS system utilizes one momentum wheel and three electromagnetic torque rods to orient the experiment viewing axis. Pointing ranges within ± 15° of vertical over the poles. Attitude knowledge accuracy computed onboard the spacecraft is better than 2° (3 sigma). The pointing strategy for SAMPEX is to point the pitch axis (i.e., the normal to the solar panels) directly at the Sun. Then the yaw axis (parallel to the detector bore sights) rotates about the pitch axis once per spacecraft orbit. The spacecraft views north over the north pole, south over the south pole, and parallel to the equator during the equatorial plane crossings (see Figure 19).

The once-per-orbit rotation mode was used from launch through May 1994. At that time, at the request of the science team, the Flight Software was modified so as to point the spacecraft in the general direction of *perpendicular* to the model Earth's magnetic field when the model field strength was <0.3 gauss. At SAMPEX altitudes, this algorithm corresponds to regions near the equator, and was chosen to increase the efficiency with which the sensors view the trapped ion populations, in particular the trapped Anomalous Cosmic Rays. This new pointing algorithm was put into use in May 1994.

After exhaustion of the HILT isobutane supply in late 1995, the spacecraft pointing requirement to avoid the ram direction was no longer necessary. This allowed a new pointing mode to be used that would greatly increase the pitch angle coverage of the sensors. In this new mode, the spacecraft continually spins at 1 RPM around the y-axis (sun pointing axis). After some initial tests, the spacecraft was put into 1 RPM mode on May 8, 1996, and is currently (October 1997) in that mode. The option remains to return to either of the previously developed pointing modes if science requirements so dictate.

An Attitude Control Electronics (ACE) box which contains signal conditioning electronics and an independent analog safehold mode controls the ACS sensor and hardware discussed previously. The onboard data system performs closed loop real-time attitude determination and control processing. Three-axis attitude determination is provided by comparing the locally measured sun vector and magnetic field vector with an on-board ephemeris model. Digital control of the spacecraft attitude is completed by sending appropriate command signals across the spacecraft data bus to the actuators.

Thermal subsystem

The thermal subsystem maintains internal SAMPEX temperatures between -10° and 50° C (Celsius). These temperatures are controlled by selected surface-finish application, regulating conduction paths, passive thermal control elements, and thermostatically-controlled heaters.

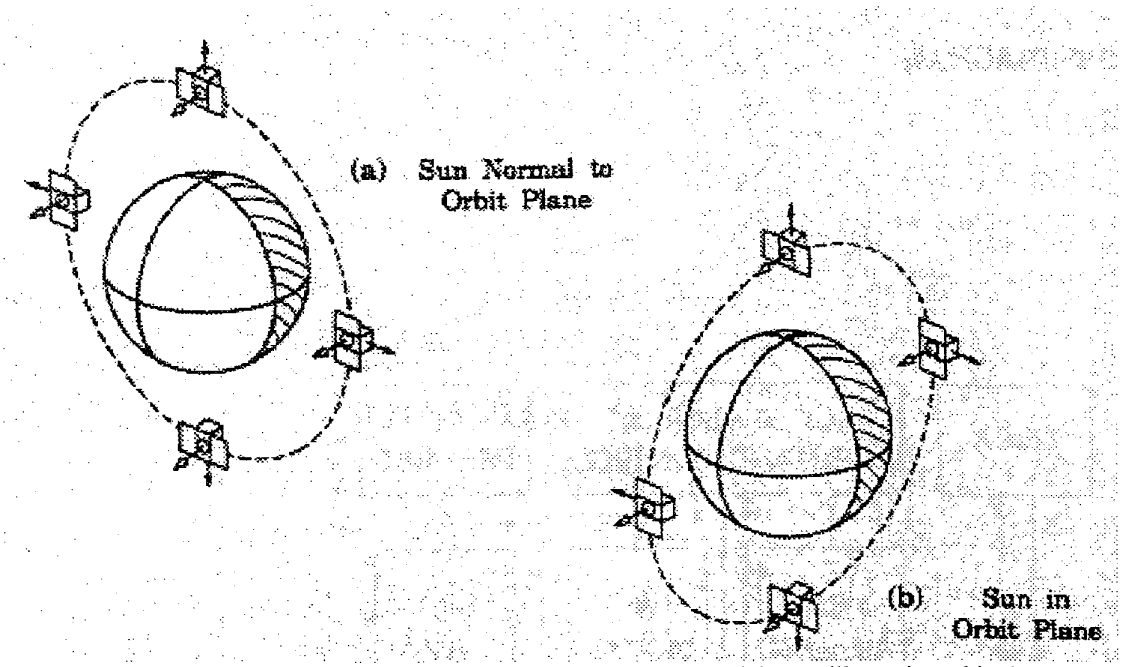

Figure 19 The initial pointing strategy for the SAMPEX spacecraft in two illustrative orbit planes.

Antenna system

The SAMPEX antenna system is composed of two quadrifilar helices, two 90° hybrid junctions, and a power divider. These omnidirectional antennas are located on the top and on the bottom of the spacecraft. The top antenna is a half-turn quadrifilar with a 150° beam width. The bottom antenna is a three-turn quadrifilar with a 210° beamwidth. Each antenna is fed with a 90° hybrid junction to create the proper phasing between elements. A power divider feeds each hybrid junction with a signal of equal amplitude and phase. This system is designed to operate over a 2025-2300 MHz frequency range. The Communications subsystem consists of a near-Earth S-band transponder operating in full duplex mode, providing reception of uplinked commands, transmission of telemetry data, and support of tracking by the designated ground station. The command data rate is 2 kb/sec. The telemetry output signal from the transmitter is modulated onto the carrier to produce the downlink signal. The transmitter modulation bandwidth is 10 MHz and its output power is 5 watts. The transponder interfaces with the antennas and the Command and Data Handling (C&DH) subsystem.

Command and Data Handling

The SAMPEX C&DH functions are performed by the Small Explorer Data System (SEDS). The SEDS provides onboard computers that can be programmed to perform mission unique functions as required and provides autonomous operation of the spacecraft when it is not in contact with the ground. The SEDS is responsible for the command and data handling functions of the SAMPEX spacecraft. The SEDS provides data collection from the different subsystems and instruments, stores the data, processes it, and sends it to the ground. The data system uses solid-state memory instead of conventional tape recorders to record spacecraft telemetry data when the spacecraft is not in contact with the ground. Data transmitted from SEDS to the ground is formatted as a "Packet Telemetry" stream in accordance with the Consultative Committee for Space Data Systems (CCSDS) and Goddard Space Flight Center standards. The SEDS is comprised of three main components:

- 1. The Recorder/Processor/Packetizer (RPP) provides storage for 26.5 Mbytes of data, packetizes commands and telemetry, and is used as a general purpose processor. The RPP supports overall spacecraft control functions and specific requirements such as attitude control. The RPP generates the telemetry data stream for transmission to the ground.

- 2. The Command Telemetry Terminal (CTT) connects the SEDS to the transponder, provides uplink command processing, downlink telemetry encoding, time code management, local telemetry acquisition and command distribution, housekeeping, attitude determination, and system monitoring functions. The CTT can control some of the spacecraft functions if the RPP fails.

- 3. The Military Standard (MIL-STD) 1773 data bus connects SEDS components to the attitude control and power subsystems. The MIL-STD-1773 bus in the implementation of the MIL-STD-1553 military avionics protocol. The 1773 bus uses optical fiber links for a high throughput and low-mass spacecraft harness. It also is a nonconductor so it cannot introduce electronic or radio frequency interference

into the system. This fiber optics approach provides spaceflight experience for a new generation of high data rate busses.

These components are used for command reception, telemetry transmission and tracking. The SAMPEX operating radio frequency modes are high- and low-rate modes. Both modes consist of coherent tracking, which provides two-way Doppler and range data, simultaneously with telemetry and command.

Examples of post launch use of the SEDS — The Small Explorer Data System (SEDS) and Attitude Control Electronics (ACE) are also very powerful and flexible systems. For example, when it was discovered post launch that the LICA high voltage power supplies drift out of control under certain conditions when the spacecraft moves through the auroral zone, the SEDS was programmed to autonomously: i) detect the LICA HV drift by comparing the HV analog readings to a limit table every 30 sec; ii) report all cases of out of limits operation; iii) immediately take corrective action if the HV supply did not return within its limits after 3 minutes (corrective action is to turn off LICA for 15 minutes, then power LICA on again and step up the HV bias voltages to their normal operating values). This procedure was put in place in November 1992, and has worked beautifully — and is an excellent solution for a difficult and possibly hazardous condition which can occur without warning on a spacecraft which is in contact with the ground only for a few minutes every several hours.

As another example, in May 1994 the pointing algorithm of the spacecraft was changed so that in equatorial regions, the spacecraft points perpendicular to the local magnetic field, and in other regions it points generally parallel to the field (while simultaneously meeting other constraints such as avoiding pointing in the ram direction, and maintaining the solar panels within 3° of perpendicular to the sun). This requires a modification in the pointing scheme twice an orbit — i.e. about every 45 minutes. Implementing such a scheme would be difficult if done by hand, but since the SAMPEX SEDS and ACE carry the pointing program and a multipole magnetic field model of the Earth, it required only a relatively simple software change to carry out this modification, and change the pointing vector calculation when the model field magnitude dropped below a limit (~0.3 gauss). *These examples illustrate the power and flexibility of the SAMPEX design, and ensure that future data collection and instrument operation can be optimized as conditions require.*

Spacecraft Status

SAMPEX launch and orbital data are in Table 4:

Table 4 — Orbit

Launch: 3 July 1992
Inclination: 82°
Initial apogee, perigee: 675 × 512 km
predicted re-entry: February 2002

Spacecraft status is nominal in all respects, with no known problems. Particular items of importance from the latest flight operations team report:

- Solar array status: will probably exceed drag lifetime; current output is 240W, load is 100W
- Battery status: operation nominal, but impossible to predict with certainty. Some trends show increase in voltage difference between top and bottom half of battery, but significance is unknown. No short term problems anticipated.

5. DATA ANALYSIS

All SAMPEX science data is sent electronically to the University of Maryland Science Operations Center (UMSOC), which receives 24 hour runs one day behind real time. Data volume is 30 Mb/day average; 50 mB day peak during large solar particle events.

UMSOC programs archive the data and produce an output data set for each day that includes extensive information on the spacecraft position and attitude, and on the geomagnetic field. A single output data set is produced that contains all experiment data, and copies are distributed to each co-investigator institution and simultaneously to the NSSDC on optical disk media. For unusual situations such as the geomagnetic storm periods in January, February, and April 1997, this "level-1" data is made available to the team electronically.

Further analysis is carried out at the investigator sites. The SAMPEX science team meets regularly to discuss data analysis issues, and also has splinter meetings to discuss analysis issues affecting only a subgroup of the team. In addition, the group often meets informally at scientific meetings.

Data Sharing

The SAMPEX science team has been active in taking advantage of world-wide-web technology to increase public access to the data set, and has had a web page in place since early 1995 (http://lepsam.gsfc.nasa.gov/www/sampex.html). The SAMPEX web page includes:

- complete instrument and mission descriptions and figures
- global electron maps for selected periods
- monthly plots of fluxes over the polar caps
- summaries of scientific results
- bibliography
- special sections, e.g. for the January and April 1997 CME driven events

We are continually working to improve the usefulness of the WWW page for both public access and research community access. For example, we recently added data taken during SAMPEX and the FAST satellite conjunctions (Figure 19).

Other data submissions from SAMPEX include:

- NSSDC submission of count rate and flux data, for WWW access through the Space Physics Data System via the Space Physics Catalog (SPyCAT).
- Publication of count rate plots in the NOAA Solar Geophysical Data bulletin

New Investigators IDS

A number of investigators have been added to the science team since launch, and many of them provided material for this report (see acknowledgments below). SAMPEX data are part of the current NASA HQ SEC guest investigator program.

Outreach Education

SAMPEX outreach activities began with the pioneer **Cooperative Satellite Learning Project** (CSLP) at Laurel (MD) high school, beginning in 1991. CSLP has since expanded to include the other SMEX missions, and has expanded from the original site to include schools in Berkeley, CA, and Pittsburgh, PA. SAMPEX talks are given at

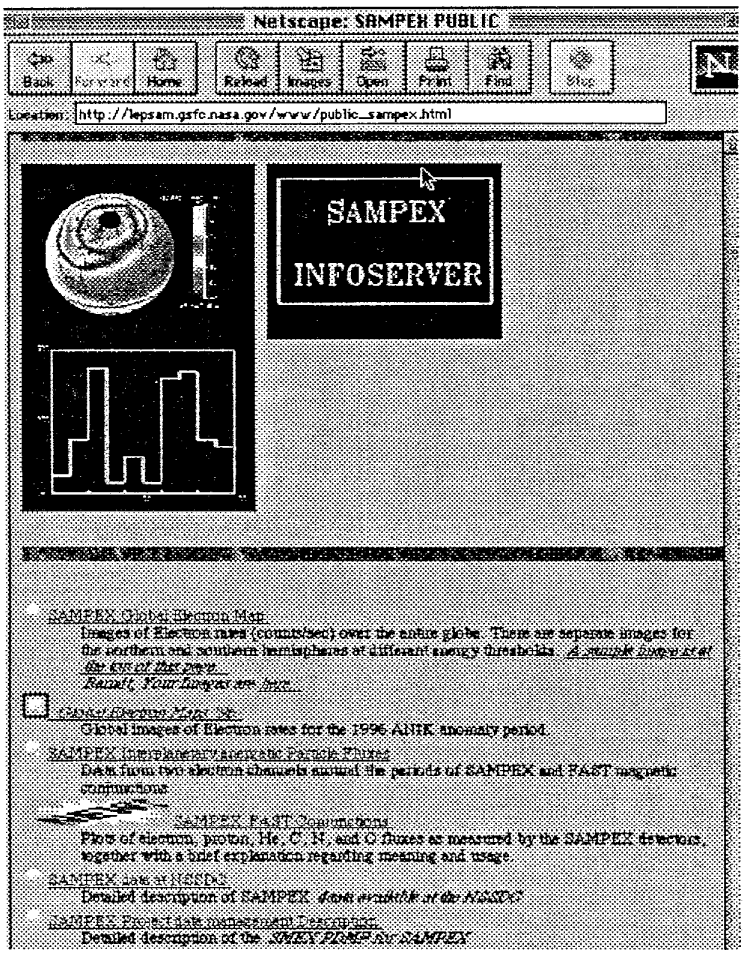

Figure 19 Header of public data section of the SAMPEX WWW site.

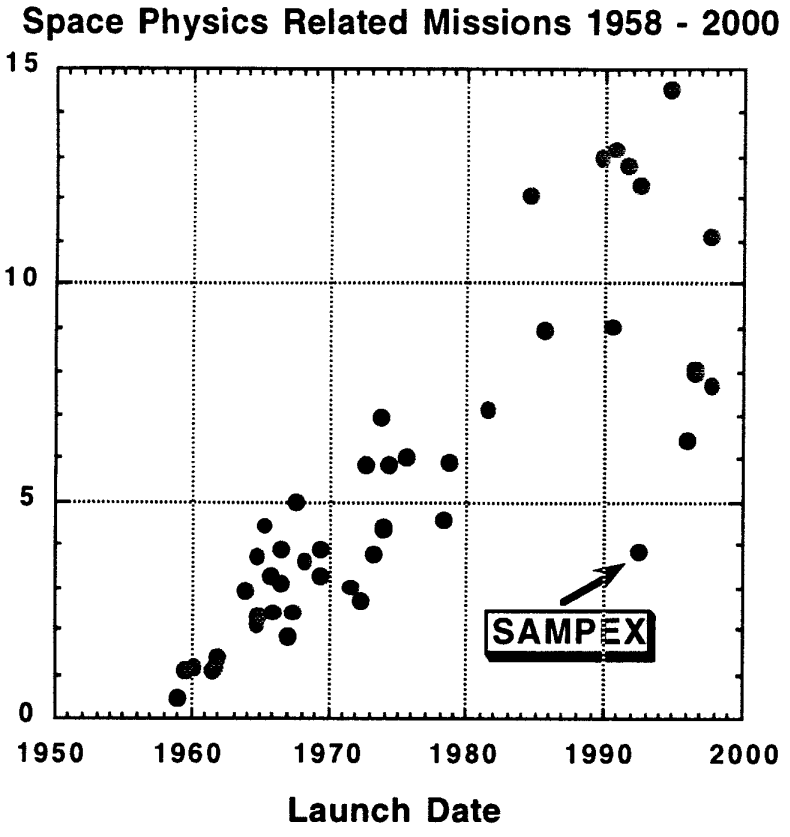

Figure 20 Launch dates of Space Physics missions [41]

Laurel, and at other school sites primarily in the Pasadena area.

At the University of Maryland **Department of Aerospace Engineering,** the **Flight Dynamics and Control Laboratory (FDCL)** is using SAMPEX data to test spacecraft attitude and control software in cooperation with the GSFC flight dynamics facility. Beginning in late 1997, the FDCL will take over responsibility for generating routine orbit products for UMSOC and the flight operations team.

Recently, a new project has begun with the **Bowie State Satellite Operations Control Center (BSSOC)** that is doing "shadow" tracking of SAMPEX from a facility in the campus library building. This project is designed to attract students into technical careers, and has the enthusiastic support of the college and students. Beginning October 1, 1997, all flight control of SAMPEX was being carried out at BSSOC.

6. CONCLUSIONS

The SAMPEX mission development was carried out successfully, meeting its original target of ~3 years from selection to launch. The time actually elapsed from the time the experimenter team was under contract to NASA till launch was about 27 months, thus meeting a key goal of the Small Explorer project to reverse a trend of increasing development times for Space Physics missions (see Fig. 20) This accomplishment was achieved only with great effort and dedication by a large number of people and organizations, including

- excellent support from the NASA Headquarters Explorer office which provided full funding for the instrument effort, and has helped to expedite many other matters,
- a tremendous commitment from NASA/Goddard, especially the Special Payloads Division, Code 700, to the SMEX project in support of the spacecraft construction, parts issues, manpower, etc.
- outstanding performance by the Small Explorer Project Office which in a short time put together an excellent managerial and technical team, whose can-do attitude resulted in an excellent spacecraft design, and whose help with e.g., parts (both electronic and mechanical) was essential on several occasions.

These organizational strengths would not have allowed SAMPEX development to proceed quickly if were it not for the revised *ground rules* being applied to the SAMPEX spacecraft. In particular, the *reporting requirements* placed on the instrument team were minimal, thanks to the Project's cooperation in substituting regular visits by the Project Instrument Manager to the sites where the flight instruments were being built. The level of *interface documentation* was kept to the minimum necessary, allowing the experimenters to concentrate on the hardware, not the paper. The product assurance approach was a breath of fresh air, especially in the electronics parts area, where the Project allowed the experimenters to use their own judgment with only advisory comments from Goddard. *Flexibility* in application of product assurance guidelines was very important: for example in the instrument data processing unit (DPU) we used hi-rel Grade "B" parts in those sections where a failure would pull down all four sensors, and generally lower grade parts in the separate sensor electronics. A full up hi-rel parts program here would have slowed our progress by a year or more,

The SAMPEX initial 3-year mission was completed in July 1995. The SAMPEX mission has been reviewed twice since launch to determine if scientific justification existed for continuing for an extended mission. The two reviews, carried out by NASA Headquarters in conjunction with other NASA flight missions, both recommended continuing SAMPEX operations and science analysis through the upcoming solar maximum. To date there have been many discoveries and "firsts" from SAMPEX studies, including:

- Determination that ACR nitrogen, oxygen, and neon are singly charged.
- Discovery that ACR oxygen, nitrogen, and neon are primarily multiply charged at energies > 15 MeV/nuc
- Discovery of the precise location of trapped anomalous cosmic rays in the magnetosphere.
- Observation of ACR oxygen to at least 1.5 GeV
- First detailed measurement of solar energetic particle isotope abundances
- Excesses (factor ~4) of neutron rich isotopes of Ne and Mg in ^{3}He-rich solar particle events.
- Discovery that magnetospheric electrons are globally accelerated in association with the impact of high speed solar wind streams, with an increasing time delay for higher energies and lower L values
- Discovery that the inner radiation belt at L=1.2 contains rare isotopes ^{2}H and ^{3}H, and roughly equal amounts of ^{3}He and ^{4}He at 10 MeV/nuc.
- Evidence that relativistic precipitating electrons provide a significant source of odd nitrogen to the middle atmosphere and can affect middle atmospheric ozone.
- Discovery that in low Earth orbit over the polar cap, albedo particles >15 MeV are more intense from below and horizontally than from above.

These have been reported in a large number of refereed journal articles and contained in reports at scientific meetings.

ACKNOWLEDGMENTS

It is a pleasure to acknowledge the enthusiastic, imaginative, and dedicated support of the Goddard Space Flight Center SMEX project in the design of the SAMPEX spacecraft, which went from selection to Critical Design Review in 15 months. The SAMPEX instrument development is supported by NASA contract NAS5-30704 and by the Bundesministerium für Forschung und Technologie, Federal Republic of Germany, contract 01OC9002. Post launch data analysis has been supported by NASA grant NAG 5-2963.

REFERENCES

[1] Baker, D.N., J.B. Blake, L.B. Callis, J.R. Cummings, S. Kanekal, B. Klecker, R.A. Mewaldt, and R.D. Zwickl, Relativistic electron acceleration and decay time scales in the inner and outer radiation belts: SAMPEX, *Geophys. Res. Letters, 21* , 409-412, 1994.

[2] Vampola, A.L., Electron pitch angle scattering in the outer zone during magnetically disturbed times, *J. Geophys. Res., 76* , 4685, 1971.

[3] Baker, D.N., J.B. Blake, L.B. Callis, J.R. Cummings, D. Hovestadt, S. Kanekal, B. Klecker, and R. Nakamura, *New magnetospheric results from the SAMPEX mission,* in *Earth's Trapped Particle Environment,* G. Reeves, Editor. 1994, American Institute of Physics: New York.

[4] Baker, D.N., J.B. Blake, S. Kanekal, B. Klecker, and G. Rostoker, Relativistic magnetospheric electron effects on Anik E and Intelsat K spacecraft operations: SAMPEX results, *EOS, Trans. Am. Geophys. U., 75 (35)*, August 30, 1994, p. 401, 1994.

[5] Li, X. and D.N. Baker, *Geophys. Res. Lett., in press* , 1997.

[6] Callis, L.B. and J.E. Nealy, Solar UV variability and its effect on stratospheric thermal structure and trace constituents, *Geophys. Res. Lett., 5* , 249, 1978.

[7] Callis, L.B., D.N. Baker, J.B. Blake, J.D. Lambeth, R.E. Boughner, M. Natarajan, R.W. Klebesadel, and D.J. Gorney, Precipitating relativistic electrons: Their long-term effect on stratospheric odd nitrogen levels, *J. Geophys. Res., 96* , 2939, 1991.

[8] Callis, L.B., R.E. Boughner, M. Natarajan, J.D. Lambeth, D. N. Baker, and J.B. Blake, Ozone depletion in the high latitude lower stratosphere:1979--1990, *J. Geophys. Res., 96* , 2921, 1991.

[9] Thorne, R.M., Energetic radiation belt precipitation: A natural depletion mechanism for stratospheric ozone, *Science, 21* , 287, 1977.

[10] Thorne, R.M., The importance of energetic particle precipitation on the chemical composition of the middle atmosphere, *PAGEOPH, 118* , 128, 1980.

[11] Baker, D.N., J.B. Blake, D.J. Gorney, P.R. Higbie, R. W., Klebesadel, and J.H. King, Highly relativistic magnetospheric electrons: A role in coupling to the middle atmosphere, *Geophys. Res. Lett., 14* , 1027, 1987.

[12] Herrero, F.A., D.N. Baker, and R.A. Goldberg, Rocket measurements of relativistic electrons: New features in fluxes, spectra, and pitch angle distributions, *Geophys. Res. Lett., 18* , 1481, 1991.

[13] Callis, L.B., R.E. Boughner, D.N. Baker, R.A. Mewaldt, J.B. Blake, R.S. Selesnick, J.R. Cummings, M. Natarajan, G.M. Mason, and J.E. Mazur, Precipitating electrons: evidence for effects on mesospheric odd nitrogen, *Geophys. Res. Lett., 23* , 1901-1904, 1996.

[14] Selesnick, R.S. and R.A. Mewaldt, Atmospheric production of radiation belt light isotopes, *J. Geophys. Res., 101* , 19745-19757, 1996.

[15] Looper, M.D., J.B. Blake, J.R. Cummings, and R.A. Mewaldt, SAMPEX observations of energetic hydrogen isotopes in the inner zone, *Radiation Meas., 26* , 967-978, 1996.

[16] Greenspan, M.E., J.E. Mazur, and G.M. Mason, SAMPEX measurements of equatorial signatures during magnetic storms, *Trans. Am. Geophys. U., 77* , F600, 1996.

[17] Leske, R.A., J.R. Cummings, R.A. Mewaldt, E.C. Stone, and T.T. von Rosenvinge, Measurements of the ionic charge states of solar energetic particles using the geomagnetic field, *Astrophys. J. (Letters), 452* , L149-L152, 1995.

[18] Baker, D.N., J.B. Blake, L.B. Callis, D. Hovestadt, B. Klecker, and S. Kanekal, Strong electron acceleration in the Earth's magnetosphere, *Adv. Space Res., in press* , 1997.

[19] Baker, D.N., *et al.*, Recurrent geomagnetic storms and relativistic electron enhancements in the outer magnetosphere: ISTP coordinated measurements, *J. Geophys. Res., in press* , 1997.

[20] Baker, D.N., T. Pulkkinen, X. Li, S.G. Kanekal, J.B. Blake, R.S. Selesnick, M.G. Henderson, G.D. Reeves, H.E. Spence, and G. Rostoker, Coronal mass ejections, magnetic clouds, and relativistic magnetospheric electrons: ISTP, *J. Geophys. Res., submitted* , 1997.

[21] Luhn, A., B. Klecker, D. Hovestadt, G. Gloeckler, F.M. Ipavich, M. Scholer, C.Y. Fan, and L.A. Fisk, Ionic charge states of N, Ne, Mg, Si, and S in solar energetic particle events, *Adv. Space Res., 4* , 161-164, 1984.

[22] Adams, J.H., Jr., R. Beaujean, P.R. Boberg, N.L. Grigorov, M.A. Kondratyeva, G.M. Mason, R.E. McGuire, R.A. Mewaldt, M.I. Panasyuk, C.A. Tretyakova, A.J. Tylka, and D.A. Zhuravlev, Determining the charge states of solar energetic ions during large geomagnetic storms, *Adv. Space Res., 13 (9)* , 367-370, 1993.

[23] Boberg, P.R., A.J. Tylka, and J. Adams, J. H., Solar energetic Fe charge state measurements: implications for acceleration by coronal mass ejection-driven shocks, *Astrophys. J. (Letters), 471* , L65-L78, 1996.

[24] Mason, G.M., J.E. Mazur, M.D. Looper, and R.A. Mewaldt, Charge state measurements of solar energetic particles observed with SAMPEX, *Astrophys. J., 452* , 901-911, 1995.

[25] Oetliker, M., B. Klecker, D. Hovestadt, G.M. Mason, J.E. Mazur, R.A. Leske, R.A. Mewaldt, J.B. Blake, and M.D. Looper, The ionic charge of solar energetic particles with energies of 0.3-70 MeV/nucleon, *Astrophys. J., 477* , 495-501, 1997.

[26] Luhn, A., D. Hovestadt, B. Klecker, M. Scholer, G. Gloeckler, F.M. Ipavich, A.B. Galvin, C.Y. Fan, and L.A. Fisk, The mean ionic charges of N, Ne, Mg, Si, and S in solar energetic particle events, *Proc. 19th Internat. Cosmic Ray Conf. (La Jolla),4*, 241-244, 1985.

[27] Ruffolo, D., Charge states of solar cosmic rays and constraints on acceleration times and coronal transport, *Astrophys. J., in press* , 1997.

[28] Fisk, L.A., B. Kozlovsky, and R. Ramaty, An interpretation of the observed oxygen and nitrogen enhancements in low-energy cosmic rays, *Astrophys. J. (Letters), 190* , L35-L37, 1974.

[29] Adams, J.H., Jr., M. Garcia-Munoz, N.L. Grigorov, M.A. Kondratyeva, G.M. Mason, R.E. McGuire, R.A. Mewaldt, M.A. Panasyuk, C.A. Tretyakova, A.J. Tylka, and D.A. Zhuravlev, The charge state of the anomalous component of cosmic rays, *Astrophys. J. (Letters), 375* , L45-L48, 1991.

[30] Klecker, B., M.C. McNab, J.B. Blake, D. Hovestadt, H. Kästle, D.C. Hamilton, M.D. Looper, G.M. Mason, J.E. Mazur, and M. Scholer, Charge state of anomalous cosmic ray nitrogen, oxygen, and neon: SAMPEX observations, *Astrophys. J. (Letters), 442* , L69-L72, 1995.

[31] Mewaldt, R.A., R.S. Selesnick, J.R. Cummings, E.C. Stone, and T.T. von Rosenvinge, Evidence for multiply charged anomalous cosmic rays, *Astrophys. J. (Letters), 466* , L43-L46, 1996.

[32] Jokipii, J.R., Constraints on the acceleration of anomalous cosmic rays, *Astrophys. J. (Lett.), 393* , L41-L43, 1992.

[33] Klecker, B., The anomalous component of cosmic rays in the 3-D heliosphere, *Space Sci. Rev., 72* , 419, 1995.

[34] Cummings, J.R., A.C. Cummings, R.A. Mewaldt, R.S. Selesnick, E.C. Stone, and T.T. von Rosenvinge, New evidence for anomalous cosmic rays trapped in the magnetosphere, *Geophys. Res. Letters, 20* , 2003-2006, 1993.

[35] Baker, D.N., G.M. Mason, O. Figueroa, G. Colon, J.G. Watzin, and R.M. Aleman, An overview of the solar, anomalous, and magnetospheric particle explorer (SAMPEX) mission, *IEEE Trans. Geosci. and Remote Sensing, 31* , 531-541, 1993.

[36] Cook, W.R., A.C. Cummings, J.R. Cummings, T.L. Garrard, B. Kecman, R.A. Mewaldt, R.S. Selesnick, E.C. Stone, D.N. Baker, T.T. von Rosenvinge, J.B. Blake, and L.B. Callis, PET: A Proton/Electron Telescope for Studies

of Magnetospheric, Solar, and Galactic Particles, *IEEE Trans. Geosci. and Remote Sens., 31* , 565-571, 1993.

[37] Cook, W.R., A.C. Cummings, J.R. Cummings, T.L. Garrard, B. Kecman, R.A. Mewaldt, R.S. Selesnick, E.C. Stone, and T.T. von Rosenvinge, MAST: A Mass Spectrometer Telescope for Studies of the Isotopic Composition of Solar, Anomalous, and Galactic Cosmic Ray Nuclei, *IEEE Trans. Geosci. and Remote Sens., 31* , 557-564, 1993.

[38] Klecker, B., D. Hovestadt, M. Scholer, H. Arbinger, M. Ertl, H. Kästle, E. Künneth, P. Laeverenz, E. Seidenschwang, J.B. Blake, N. Katz, and D.J. Mabry, HILT: A Heavy Ion Large Area Proportional Counter Telescope for Solar and Anomalous Cosmic Rays, *IEEE Trans. Geosci. and Remote Sens, 31* , 542-548, 1993.

[39] Mabry, D.J., S.J. Hansel, and J.B. Blake, The SAMPEX data Processing Unit (DPU), *IEEE Trans. Geosci. and Remote Sens., 31* , 572-574, 1993.

[40] Mason, G.M., D.C. Hamilton, P.H. Walpole, K.F. Heuerman, T.L. James, M.H. Lennard, and J.E. Mazur, LEICA: a low energy ion composition spectrometer for the study of solar and magnetospheric heavy ions, *IEEE Trans. Geosci. and Remote Sensing, 31* , 549-556, 1993.

[41] Williams, D.J., *A Space Physics Paradox*. 1994, National Research Council:

BIOGRAPHY

Glenn Mason *received his A.B. in Physics from Harvard College in 1965, and his Ph.D. in Physics from the University of Chicago in 1971. Dr. Mason is Professor jointly in the Department of Physics and the Institute for Physical Science and Technology at the University of Maryland, College Park. He has worked on the development of novel instrumentation that allows determination of the mass composition of solar and interplanetary particles in previously unexplored energy ranges. His research work has included galactic cosmic rays, solar energetic particles, and the acceleration and transport of particles both in the solar atmosphere and in the interplanetary medium. He is Principal Investigator on the NASA Solar, Anomalous, and Magnetospheric Explorer (SAMPEX) spacecraft mission, and is co-investigator on energetic particle instruments for the NASA Wind spacecraft, and the NASA Advanced Composition Explorer (ACE) spacecraft. He is currently Chair of the NASA Sun-Earth Connections Advisory Subcommittee (SECAS), is a member of the NASA Space Science Advisory Committee (SScAC), and the Steering Committee of the Space Science Working Group of the Association of American Universities.*